Manganese(II) and Gadolinium(III) Complexes with New 13- and 16-Membered Dioxopolyazacycloalkanes Having Pendant Hydroxy and Carboxymethyl Groups

Michiko B. Inoue,[†,‡] Rosa Elena Navarro,[†] Motomichi Inoue,*[,†] and Quintus Fernando[‡]

CIPM, Universidad de Sonora, Apartado Postal 130, Hermosillo, Sonora, Mexico, and Department of Chemistry, University of Arizona, Tucson, Arizona 85721

Received June 15, 1995[⊗]

New 13-membered and 16-membered functionalized macrocycles, dioxopolyazacycloalkanes with pendant hydroxy and carboxymethyl groups, have been synthesized: the 13-membered macrocycle is 12-hydroxy-2,9-dioxo-1,4,7,-10-tetraaza-4,7-cyclotridecanediacetic acid [abbreviated as (13edtapnOH)H_2] and the 16-membered macrocycle is 15-hydroxy-2,12-dioxo-1,4,7,10,13-pentaaza-4,7,10-cyclohexadecanetriacetic acid [(16dtpapnOH)H_3]. The resulting macrocycles have been characterized by ^{1}H NMR at different pD values, and the protonation sites and the proton populations have been determined for each protonation step. Nonionic Mn^{2+} and Gd^{3+} complexes with these ligands, [Mn(13edtapnOH)(H_2O)]·3H_2O and [Gd(16dtpapnOH)(H_2O)]·3H_2O, have been characterized by single-crystal X-ray analyses. The Mn^{2+} complex crystallized in the triclinic space group $P\bar{1}$ with a = 11.453(1) Å, b = 12.432(1) Å, c = 14.432(2) Å, α = 77.39(1)°, β = 76.24(1)°, γ = 88.50(1)°, and Z = 4. The unit cell contains two types of metal chelate molecules: one has a six-coordination geometry described by a quasi-trigonal prism and the other has a seven-coordination geometry described by a distorted capped trigonal prism. The formation of the two types of Mn^{2+} chelate molecules arises from interaction between an OH oxygen and an amide nitrogen in a coordinated ligand molecule. The Gd^{3+} complex crystallized in the monoclinic space group Pc with a = 8.405(2) Å, b = 9.688(3) Å, c = 16.392(4) Å, β = 109.117(3)°, and Z = 2. The coordination geometry of the Gd^{3+} complex is a tricapped trigonal prism. The electron paramagnetic resonance hyperfine structure of the Mn^{2+} complex in a glass matrix showed the so-called forbidden-transition ($\Delta m_I = \pm 1$) lines at intermediate fields between the allowed-transition ($\Delta m_I = 0$) lines. The NMR T_1 and T_2 relaxivities of the Gd^{3+} complex in 90% D_2O were determined to be r_1 = 3.45 s^{-1} mM^{-1} and r_2 = 4.4 s^{-1} mM^{-1} at 250 MHz. The ^{1}H NMR spectra of the free ligands show that the introduction of an OH group increases the rigidity of the ring systems, owing to interaction between the hydroxy and amide groups. This interaction is responsible in part for the structural and solution properties of the metal chelates.

Introduction

The synthesis of highly functionalized macrocyclic receptors is an important initial step in the investigation of molecular recognition properties of these large ring compounds.[1] The synthesis and characterization of macrocycles that have different types of coordinating groups are the main objectives in a series of our continuing studies.[2−7] Condensation reactions between a diamine and ethylenediaminetetraacetic (edta) dianhydride or diethylenetriaminepentaacetic (dtpa) dianhydride give dioxopolyazacycloalkanes with different ring sizes and with a different number of pendant carboxymethyl groups.[2,4,8,9] The use of 1,3-diaminopropane (pn) as a diamine gives 13-membered and 16-membered macrocycles, (13edtapn)H_2 (**I**) and (16dtpapn)H_3 (**II**).[3,4] These macrocyclic ligands form nonionic metal chelates with bivalent and trivalent metal ions, respectively. Single-crystal X-ray analyses of the resulting metal complexes have shown the formation of a novel coordination geometry around a central metal ion as a consequence of the introduction of amide groups in the ring system.[2−7] The partial double-bond character of the C−N bond in an amide group decreases the flexibility of the macrocyclic ring and defines the conformation of the ligands. When an additional functional group is introduced in the new series of macrocycles, the resulting macrocycles are expected to have a higher steric constraint.

In this work, we have carried out condensation reactions by using 1,3-diamino-2-hydroxypropane (pnOH) as a diamine and obtained new 13-membered and 16-membered dioxopolyazacycloalkane polyacetic acids, (13edtapnOH)H_2 (**III**) and (16dtpapnOH)H_3 (**IV**), that incorporate a hydroxy group as an additional pendant functional group. These new macrocycles have been characterized by ^{1}H NMR at different pD values. Their nonionic chelates of Mn^{2+} and Gd^{3+}, Mn(13edtapnOH) and Gd(16dtpapnOH), have been characterized by X-ray crystal analyses because these metal ions, which have no crystal-field stabilization energies in the high-spin state, are suitable for studying the effect of ligand conformation on coordination

[†] Universidad de Sonora.
[‡] University of Arizona.
[⊗] Abstract published in *Advance ACS Abstracts,* November 1, 1995.

(1) (a) Izatt, R. M., Christensen, J. J., Eds. *Synthesis of Macrocycles, The Design of Selective Complexing Agents*; Progress in Macrocyclic Chemistry Vol. 3; John Wiley & Sons: New York, 1987. (b) Hancock, R. D.; Martell, A. E. *Chem. Rev.* **1989**, *89*, 1875. (c) Izatt, R. M.; Pawlak, K.; Bradshaw, J. S.; Bruening, R. L. *Chem. Rev.* **1991**, *91*, 1721. (d) van Veggel, F. C. J. M.; Verboom, W.; Reinhoudt, D. N. *Chem. Rev.* **1994**, *94*, 279. (e) Alexander, V. *Chem. Rev.* **1995**, *95*, 273.
(2) Inoue, M. B.; Villegas, C. A.; Asano, K.; Nakamura, M.; Inoue, M.; Fernando, Q. *Inorg. Chem.* **1992**, *31*, 2480.
(3) Inoue, M. B.; Fernando, Q.; Villegas, C. A.; Inoue, M. *Acta Crystallogr., Sect. C* **1993**, *49*, 875.
(4) Inoue, M. B.; Inoue, M.; Muñoz, I. C.; Bruck, M. A.; Fernando, Q. *Inorg. Chim. Acta* **1993**, *209*, 29.
(5) Inoue, M. B.; Inoue, M.; Fernando, Q. *Inorg. Chim. Acta* **1993**, *209*, 35.
(6) Inoue, M. B.; Oram, P.; Inoue, M.; Fernando, Q.; Alexander, A. L.; Unger, E. C. *Magn. Reson. Imaging* **1994**, *12*, 429.
(7) Inoue, M. B.; Inoue, M.; Fernando, Q. *Acta Crystallogr., Sect. C* **1994**, *50*, 1037.
(8) Carvalho, J. F.; Kim, S.-H.; Chang, C. A. *Inorg. Chem.* **1992**, *31*, 4065.
(9) Franklin, S. J.; Raymond, K. N. *Inorg. Chem.* **1994**, *33*, 5794.

0020-1669/95/1334-6074$09.00/0

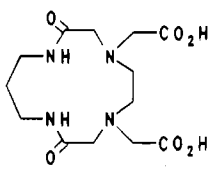

I (13edtapn)H_2

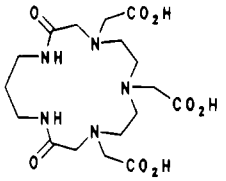

II (16dtpapn)H_3

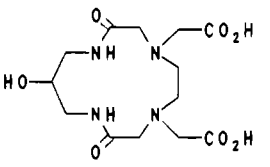

III (13edtapnOH)H_2

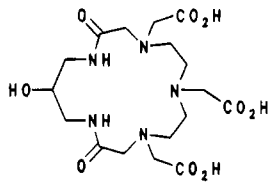

IV (16dtpapnOH)H_3

geometries. Moreover, highly stable nonionic chelates of Gd^{3+} with macrocyclic ligands are expected to be potentially useful magnetic resonance imaging agents.[10]

Experimental Section

Syntheses of Macrocycles. A sample of (13edtapnOH)H_2 was synthesized by a condensation reaction between edta dianhydride (Aldrich) and 1,3-diamino-2-hydroxypropane (Aldrich). A 0.72 g (8 mmol) sample of the diamine dissolved in 60 mL of dry dimethylformamide (DMF) was added dropwise to 2.05 g (8 mmol) of edta dianhydride in 300 mL of DMF, with vigorous stirring during a 2 h period under a nitrogen atmosphere. The resulting reaction mixture was allowed to stand overnight. The colorless solid formed was removed by filtration. The filtrate was concentrated to approximately 15 mL with a rotary evaporator and was mixed with approximately 15 mL of methanol. The colorless solid formed was removed again by filtration, and the resulting yellowish solution was concentrated to a viscous liquid, which was diluted with 5 mL of water and mixed with 5 mL of methanol. The compound crystallized in a few days from the resulting solution. Yield: 20%. Decomp temp: 222 °C. Anal. Calcd for $C_{13}H_{22}N_4O_7$: C, 45.08; H, 6.40; N, 16.18%. Found: C, 44.94; H, 6.50; N, 16.73 (the elemental analyses were performed by Desert Analytics, Tucson, AZ). ^{1}H NMR: See Figure 1.

A sample of (16dtpapnOH)H_3 was prepared by a condensation reaction between dtpa dianhydride and 1,3-diamino-2-hydroxypropane. A 0.8 g sample of the diamine in 100 mL DMF was added dropwise to 3.03 g of dtpa dianhydride (Sigma) in 300 mL DMF with vigorous stirring under a nitrogen atmosphere. Any solid formed was removed by filtration. The filtrate was concentrated to an oil by a rotary evaporator. When tetrahydrofuran was added to the oil, a colorless solid was obtained. The product was suspended in water, and the colorless solid was separated by filtration from a yellow solution, washed successively with water and acetone, and dried in vacuum. Yield: 20%. Melting point: 184−185 °C (decomp). Anal. Calcd for $C_{17}H_{29}N_5O_9 \cdot H_2O$: C, 43.86; H, 6.71; N, 15.05%. Found: C, 43.54; H, 6,73; N, 14.67%. ^{1}H NMR: See Figure 2.

Syntheses of Metal Complexes. Mn(13edtapnOH)·$2H_2O$ was prepared by a reaction between (13edtapnOH)H_2 and manganese(II) carbonate. Solid Mn carbonate in excess was added to the ligand (0.1 g) in water (10 mL). After the mixture was stirred overnight at a temperature of ≈40 °C, excess carbonate was removed by filtration. When ethanol was added to the filtrate, the metal complex was obtained as a colorless solid. The metal complexes were precipitated as microcrystals from an aqueous solution by adding acetone. Yield: 90%. Anal. Calcd for $MnC_{13}H_{20}N_4O_7 \cdot 2H_2O$: C, 35.87; H, 5.56; N, 12.87%. Found: C, 35.53; H, 5.53; N, 12.38%.

Gd(16dtpapnOH)·$4H_2O$ was prepared by a reaction between gadolinium(III) carbonate (Johnson Matthey, Rare Earth Products) and (16dtpapnOH)H_3. The mixture of the carbonate (50 mg) and the ligand (70 mg) in water (10 mL) was stirred overnight at ≈40 °C. The product formed was a colorless suspension, which was dissolved by adding more water at ≈40 °C. When the resulting solution was concentrated and mixed with acetone, the gadolinium(III) complex was obtained as a colorless solid. Yield: 90%. Anal. Calcd for $GdC_{17}H_{26}N_5O_9 \cdot 4H_2O$: C, 30.31; H, 5.09; N, 10.39%. Found: C, 30.38; H, 5.24; N, 9.85%.

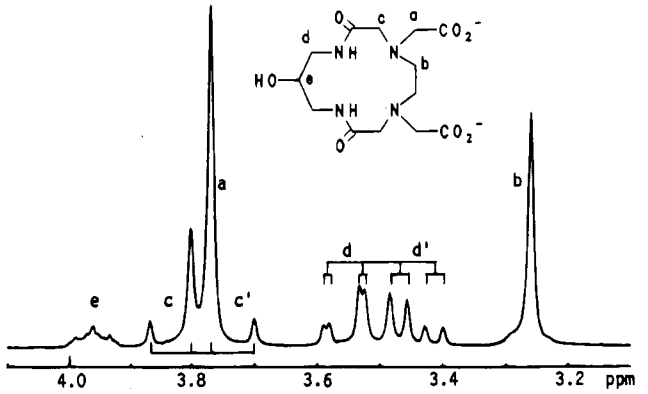

Figure 1. ^{1}H NMR spectrum of (13edtapnOH)H_2 in D_2O (pD = 3.35) referenced to DSS.

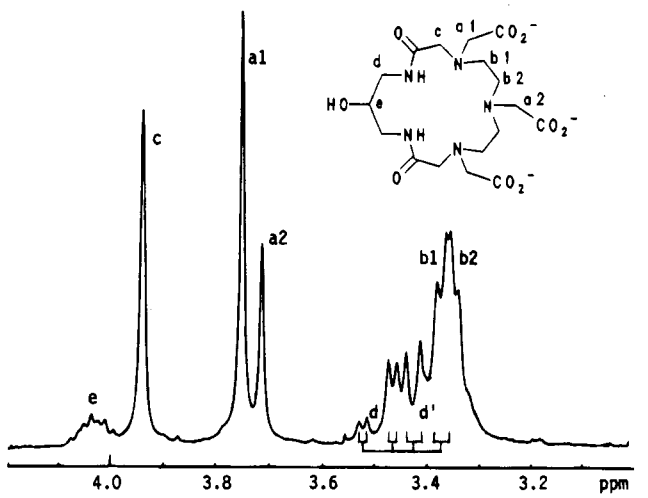

Figure 2. ^{1}H NMR spectrum of (16dtpapnOH)H_3 in D_2O (pD = 3.58) referenced to DSS.

Magnetic Resonance Measurements. The ^{1}H NMR spectra of the macrocycles in 99.9% D_2O (Cambridge Isotope Laboratories) were recorded on Bruker AM 250 and WM 250 NMR spectrometers at a probe temperature of 23 °C. The internal reference was sodium 3-(trimethylsilyl)propanesulfonate (DSS). Sample solutions with different pD values were prepared by adding dilute KOD/D_2O (prepared from an Aldrich 40% w/w solution) or dilute DCl/D_2O (prepared from an Aldrich 18% w/w solution). The sample concentration was approximately 0.01 M. The pH values of the solutions were determined with a Beckman Phi 72 pH meter equipped with an Aldrich ultrathin long stem combination electrode (with calomel reference) and converted to pD values by the equation, $pD = pH_{meas} + 0.44$.[11]

The NMR relaxation times T_1 and T_2 of Gd(16dtpapnOH)·$4H_2O$ at 250 MHz were determined with a Bruker AM 250 spectrometer at 23 °C for 90% D_2O solutions in a concentration range of 1−6 mM. The 180°−τ−90° pulse sequence technique was used for T_1 measurements and the Carr−Purcell−Meiboom−Gill method for T_2.[12] The relaxivities r_1 and r_2 were calculated from T_n (n = 1 or 2) by the equation, $T_n^{-1} = r_n[Gd] + T_{n0}^{-1}$, where [Gd] is the molar concentration and T_{n0} is T_1 or T_2 for the solvent.

(10) Lauffer, R. B. *Chem. Rev.* **1987**, *87*, 901.

(11) Mikkelsen, K.; Nielsen, S. O. *J. Phys. Chem.* **1960**, *64*, 632.

(12) Farrar, T. C.; Becker, E. D. *Pulse and Fourier Transform NMR, Introduction to Theory and Methods*; Academic Press: New York, 1971.

Table 1. Crystallographic Data for Mn(13edtapnOH)·4H_2O and Gd(16dtpapnOH)·4H_2O

	Mn(13edtapnOH)·4H_2O	Gd(16dtpapnOH)·4H_2O
formula	$[Mn(C_{13}H_{20}N_4O_7)(H_2O)]\cdot 3H_2O$	$[Gd(C_{17}H_{29}N_5O_9)(H_2O)]\cdot 3H_2O$
fw	471.33	676.76
space group	triclinic, $P\bar{1}$ (No. 2)	monoclinic, *Pc* (No. 7)
a, Å	11.453(1)	8.405(2)
b, Å	12.432(1)	9.688(3)
c, Å	14.432(2)	16.392(4)
α, deg	77.39(1)	
β, deg	76.24(1)	109.117(3)
γ, deg	88.50(1)	
V, Å^3	1947.1(4)	1261(1)
Z	4	2
T, °C	20	22
λ, Å	0.71073	0.71073
ρ_{calcd}, g cm^{-3}	1.61	1.78
μ, cm^{-1}	7.1	27.1
R^a	0.039	0.014
$R_w{}^b$	0.045	0.020

$^a R = \sum|F_o - F_c|/\sum F_o$. $^b R_w = [\sum w(F_o - F_c)^2/\sum wF_o^2]^{1/2}$.

The electron paramagnetic resonance (EPR) spectrum was observed for Mn(13edtapnOH)·2H_2O in a 50% methanol glass matrix at liquid nitrogen temperature on a Bruker ESP-300 spectrometer operating in the X band. The sample concentration was approximately 0.01 M.

X-ray Crystal Analyses. The single crystals suitable for X-ray crystal analyses were grown from aqueous solutions by slow evaporation. The data collection was performed with monochromated Mo Kα radiation (λ = 0.710 73 Å). The crystallographic data are summarized in Table 1. Scattering factors were taken from Cromer and Waber.[13] All calculations were performed on a VAX computer with the program package MolEn.[14]

A colorless crystal of Mn(13edtapnOH)·4H_2O in the shape of an oblique plate with approximate dimensions of 0.40 × 0.25 × 0.08 mm^3 was sealed in a capillary and mounted on an Enraf-Nonius CAD4 diffractometer. The crystal system was triclinic; a higher-symmetry space group could not be assumed although the number of molecules in the unit cell was four (*i.e.*, $Z = 4$). This is consistent with the solved structure, which involves two types of metal chelate molecules having different coordination geometries and hydrogen-bonding modes. A total of 6834 reflections ($+h,\pm k,\pm l$) were collected with a maximum 2θ of 50°; all the reflections were unique; 4347 reflections with $I > 3\sigma_I$ were used in the refinements. An empirical absorption correction based on a series of ψ-scans was applied using the program PSICALC. Relative transmission coefficients ranged from 0.93 to 1.00. The positions of metal atoms were located by the Patterson heavy-atom method. The remaining non-hydrogen atoms were located in succeeding difference Fourier syntheses. Hydrogen atoms bonded to oxygen and nitrogen atoms were located in difference Fourier syntheses, and those bonded to carbon atoms were placed at the idealized positions with a C−H distance of 0.95 Å. All the hydrogen atoms were constrained to ride on the atoms to which they are bonded. The final refinement converged at $R = 0.039$ with 523 parameters. The maximum and minimum peaks in the final difference map were 0.44(6) and −0.10(6) e Å^{-3}, respectively.

A colorless crystal of Gd(16dtpapnOH)·4H_2O in the shape of a plate with an approximate dimension of 0.45 × 0.37 × 0.20 mm^3 was mounted on a Syntex $P2_1$ diffractometer with a Crystal Logics computer control system. A total of 2511 reflections ($+h,+k,\pm l$) were collected with a maximum 2θ of 50°; 2369 reflections were unique; 2320 reflections with $I > 3\sigma_I$ were used in the refinements. An empirical absorption correction based on a ψ-scan was calculated using the program ABSCOR. The transmission factors ranged from 0.81 to 1.00. The position of a Gd atom was revealed by the Patterson heavy-atom method. The difference Fourier map generated with a Gd atom had a 2-fold axis on the Gd atom, and one peak in each symmetry-related pair was imaginary. The structure was solved by selecting the space group *Pc*; the alternative space group, *P2/c*, was discarded because the final molecular structure does not have 2-fold symmetry. The hydrogen atoms were included in the refinement in the manner described above for Mn(13edtapnOH)·4H_2O. The final refinement converged at $R = 0.014$ with 323 parameters. The maximum and minimum peaks in the final difference map were 0.66(5) and −0.10(5) e Å^{-3}, respectively.

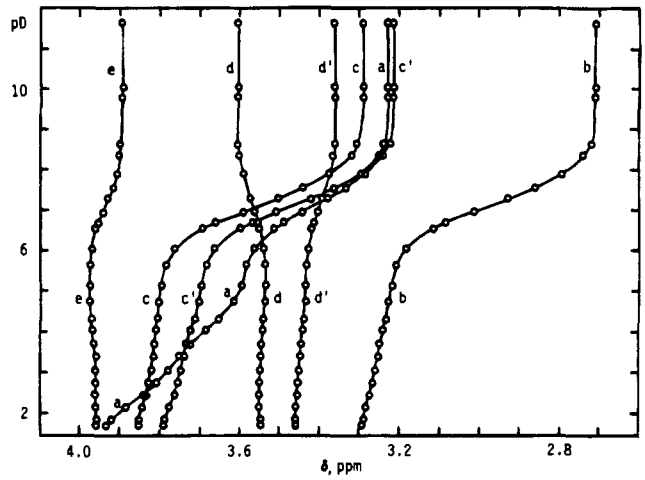

Figure 3. pD dependence of ^{1}H NMR shift δ_i (referenced to DSS) observed for (13edtapnOH)H_2. The solid lines are drawn as an aid to visualizing the trends in the chemical shift.

Results

^{1}H NMR of (13edtapnOH)H_2. The ^{1}H NMR spectrum of (13edtapnOH)H_2 and the signal assignments are shown in Figure 1. The multiplet centered at $\delta = 3.96$ is assigned to proton e on the basis of the integrated signal intensity. Two protons in the CH_2(d) group adjacent to the CH(e) group are not equivalent and show a set of signals, in the region of $\delta = 3.4-3.6$, that can be analyzed as an AB spectrum modified by the first-order coupling with proton e: $J(d - d') = 14$ Hz, $J(d - e) = 2$ Hz, and $J(d' - e) = 7$ Hz. The nonequivalence of two protons in a CH_2(d) group implies that the macrocyclic ring is rigid. A set of signals showing an AB spectrum centered at $\delta = 3.78$ with $J = 17$ Hz is, therefore, assigned to protons c and c′ that are bound to the ring framework; the singlet at $\delta = 3.76$ is assigned to proton a because the internal fluctuation of the pendant $-CH_2-CO_2^-$ group is greater than that of the framework of the ring. The remaining signal at $\delta = 3.26$ is assigned to proton b.

The pD dependence of the NMR shifts is shown in Figure 3. In a pD range of 5.5−8.5, large changes in the chemical shifts of protons a, b, and c were observed, due to the deshielding effect caused by protonation. Proton e showed a small change in its chemical shift. It is probable that the hydrogen bonds formed by the OH group are altered upon protonation. The signals of protons d and d′ shifted in the same pD region, but the averaged position of the peaks was practically unchanged. The shifts are, therefore, due to a change in the orientation of a CH_2(d) group rather than the deshielding effect caused by protonation. At pD values below ≈5, a large downfield shift was observed only for proton a. The pD profiles are consistent with the signal assignments. Although large chemical shift changes were observed upon protonation, the spin−spin coupling constants were essentially unchanged.

(13) Cromer, D. T.; Waber, J. T. *International Tables for X-ray Crystallography*, The Kynoch Press: Birmingham, England, 1974; Vol. IV, Table 2.2B.
(14) Fair, C. K. *MolEn. An Interactive Intelligent System for Crystal Structure Analysis*; Enraf-Nonius: Delft, The Netherlands, 1990.

The proton population can be calculated from a chemical shift change by assuming the following equation:[15]

$$\Delta\delta_i = \sum C_{ij} f_j(n) \qquad (1)$$

where $\Delta\delta_i$ is the chemical shift change of the ith proton (i = a, b), C_{ij} is the proton shift constant of the ith proton due to the protonation of the jth site (*i.e.*, nitrogen or oxygen atom), and $f_j(n)$ is the proton population of the jth site (or the averaged fraction of time during which the jth site is protonated) at the nth order of protonation, $\sum f_j(n) = n$. The C_{ij} value is given as $C_N = 0.75$ ppm for the protons in CH_2NR_2, $C_{N'} = 0.35$ ppm for the italicized protons in $CH_2CH_2NR_2$, and $C_O = 0.20$ ppm for protons in $CH_2CO_2^-$. Different C_{ij} values have been proposed.[16] Ambiguity in the selection of appropriate C_{ij} values results in the large uncertainty of the $f_j(n)$ values obtained. Despite the large uncertainty, the results of the calculation are useful to explain the mode of protonation. The proton population at each protonation step was, therefore, calculated in the same manner as reported for (13edtapn)H_2,[17] with the same set of C_N, $C_{N'}$ and C_O values described above. For the first protonation (*i.e.*, for the LH^- species), $f_N(1) = 0.46$ and $f_O(1) = 0.04$; for the second protonation (LH_2 species), $f_N(2) = 0.51$ and $f_O(2) = 0.49$. The first protonation occurs at an amine nitrogen atom, and the proton is shared by two equivalent $>NCH_2CO_2$ moieties *via* an intramolecular prototropy so that each amine nitrogen site carries a proton population of approximately 0.5 in the LH^- species. The succeeding protonation occurs at the acetate oxygen sites. The protonation modes are similar to those proposed for 1,4,8,11-tetraaza-1,4,8,11-cyclotetradecanetetraacetic acid.[16]

Changes in the line shape of signal b occurred at different pD values: at pD ≥ 9, an ill-defined A_2B_2 spectrum was observed; in the pD range 7−9, the structure collapsed and a broad singlet was observed; below pD ≈ 7, a sharp singlet was observed. These results indicate that the internal-fluctuation rate of an $-N-CH_2(b)-CH_2(b)-N-$ group increases with decreasing pD, *i.e.*, the ring framework becomes more flexible when protonated.

For the ^{1}H NMR spectrum of (13edtapn)H_2, two protons in every CH_2 group are equivalent in contrast to the spectrum of (13edtapnOH)H_2. The internal fluctuation of the CH_2 groups in the former macrocycle is sufficiently rapid to make two protons in the CH_2 group equivalent.[17] The introduction of an OH group in the ring system, therefore, increases the rigidity of the ring framework. On the other hand, the ^{1}H NMR spectra of (13edtapn)H_2 and (13edtapnOH)H_2 show essentially identical pD dependence; the differences of chemical shifts upon protonation and the pD regions where protonations occur are essentially the same for the two compounds. The basicities of donor atoms, therefore, are not influenced by the introduction of an OH group.

^{1}H NMR of (16dtpapnOH)H_3. Figure 2 shows the ^{1}H NMR spectrum observed for (16dtpapnOH)H_3 and the signal assignments of the protons. On the basis of the signal intensities, the multiplet centered at $\delta = 4.04$ and the singlet at $\delta = 3.72$ are assigned to protons e and a2, respectively. Protons of a CH_2-(d) group show an AB spectrum, at $\delta = 3.4-3.55$, modified by the coupling with proton e: J(d−d′) = 14 Hz, J(d−e) = 4 Hz, and J(d′−e) = 7 Hz. Protons b1 and b2 show an A_2B_2 spectrum in the region, $\delta = 3.3-3.4$; these protons were identified as shown in Figure 2 on the basis of their pD dependence. The signals at $\delta = 3.95$ and 3.76 are assignable to either protons a1 or c. The integrated intensities of these signals are identical with each other, but the 3.76 ppm signal is taller than the signal at 3.95 ppm. Because the c protons do not show an AB spectrum, in contrast to the c protons in (13edtapnOH)H_2, they undergo a rapid internal fluctuation. This fluctuation, however, is expected to be slower than that of a pendant CH_2 group, which shows a very sharp singlet due to a rapid internal fluctuation. The shorter signal at $\delta = 3.95$ is, therefore, assigned to proton c and the taller signal to proton a1.

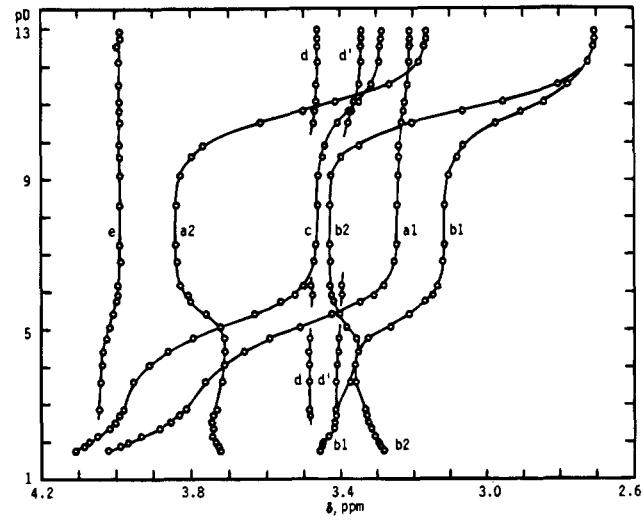

Figure 4. pD dependence of ^{1}H NMR shift δ_i (referenced to DSS) observed for (16dtpapnOH)H_3. The signals of d and d′ protons in the pD range 5−10.5 and the signal from the e protons at pD values less than 2.4 were masked by their adjacent signals. The solid lines are drawn as an aid to visualizing the trends in the chemical shift.

The pD dependence of the chemical shifts is shown in Figure 4. The signals of d and d′ protons in the pD range 5−10.5 and the signal of the e proton at pD values less than 2.4 were masked by their adjacent signals. The proton populations at each protonation stage were calculated in the same manner as described above for (13edtapnOH)H_2: for LH^{2-}, $f_{N1}(1) = 0.05$, $f_{N2}(1) = 0.90$, and $f_{O1}(1) = f_{O2}(1) = 0$; for LH_2^-, $f_{N1}(2) = 0.50$, $f_{N2}(2) = 0.65$, $f_{O1}(2) = 0.05$, and $f_{O2}(2) = 0.25$; for LH_3, $f_{N1}(3) = f_{N2}(3) = 0.60$, $f_{O1}(3) = 0.35$, and $f_{O2}(3) = 0.50$ (O1 and N1 are the protonation sites of the terminal *N*-carboxymethyl group, and O2 and N2 are sites of the central *N*-carboxymethyl group). These values clearly show the mode of protonation, despite their large uncertainties. The first protonation mainly occurs on the central amine nitrogen N2. Upon the second protonation, a redistribution of protons occurs between amine nitrogen atoms, N1 and N2, to reduce electrostatic repulsion between the attached protons. The redistribution of protons leads to the reverse chemical shifts of protons a2 and b2 in the pD range 5−6, as reported for the protonation of diethylenetriaminepentaacetate.[18] The third protonation occurs on the carboxylate oxygen atoms. The pD dependence and the mode of protonation are almost identical with those for (16dtpapn)H_3.[17] The basicities of donor atoms are not significantly influenced by the introduction of an OH group. On the other hand, the ring framework of the OH derivative is less flexible because two protons, d and d′, that belong to the same CH_2 group are not equivalent in contrast to (16dtpapn)H_3.

Structure of Mn(13edtapnOH)·4H_2O. The M−X distances and other geometrical parameters are collected in Table 2. The asymmetric unit contains two crystallographically nonequivalent

(15) Sudmeier, J. L.; Reilley, C. N. *Anal. Chem.* **1964**, *36*, 1698.
(16) Desreux, J. F.; Merciny, E.; Loncin, M. F. *Inorg. Chem.* **1981**, *20*, 987.
(17) Inoue, M. B.; Oram, P.; Inoue, M.; Fernando, Q. *Inorg. Chim. Acta* **1995**, *232*, 91.
(18) Letkeman, P.; Martell, A. E. *Inorg. Chem.* **1979**, *18*, 1284.

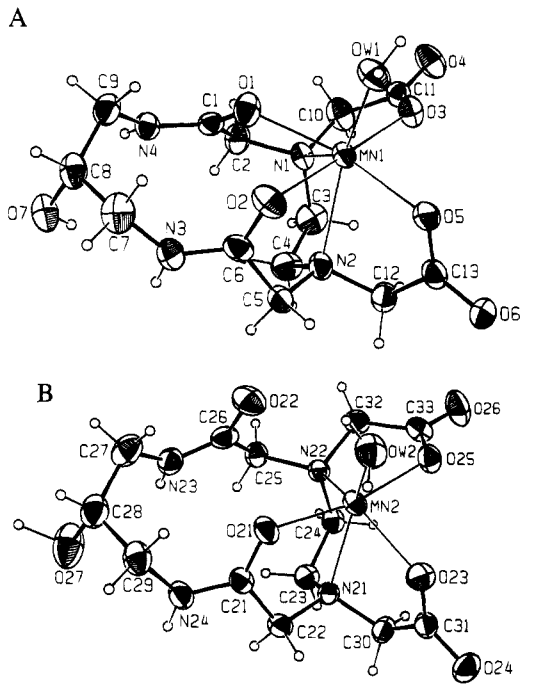

Figure 5. Structures of two [Mn(13edtapnOH)(H_2O)] molecules: (A) molecule A; (B) molecule B. The atoms are shown at a 50% probability level. The coordination geometry of molecule A is a distorted capped-trigonal prism. The Mn2−O22 distance in molecule B is 3.188 Å; six coordinated atoms in the first coordination sphere form a quasi-trigonal prism around Mn2.

Table 2. Selected Geometrical Parameters for Mn(13edtapnOH)·4H_2O

M−X Distances (Å)			
Mn1−O1$_{amide}$	2.183(3)	Mn2−O21$_{amide}$	2.113(3)
Mn1−O2$_{amide}$	2.478(3)	Mn2−O22$_{amide}$	3.188(3)
Mn1−O3$_{carboxylate}$	2.134(3)	Mn2−O23$_{carboxylate}$	2.181(2)
Mn1−O5$_{carboxylate}$	2.161(3)	Mn2−O25$_{carboxylate}$	2.128(3)
Mn1−N1$_{amine}$	2.576(3)	Mn2−N21$_{amine}$	2.359(3)
Mn1−N2$_{amine}$	2.394(3)	Mn2−N22$_{amine}$	2.374(3)
Mn1−Ow1	2.175(2)	Mn2−Ow2	2.185(3)
Bond Distances (Å) between an Amide N Atom and the Neighboring C Atoms			
N3−C6	1.317(5)	N23−C26	1.308(5)
N3−C7	1.452(5)	N23−C27	1.457(5)
N4−C1	1.317(5)	N24−C21	1.316(5)
N4−C9	1.451(5)	N24−C29	1.453(5)
Interatomic Distances (Å) between Hydroxy O and Amide N Atoms			
O7−N3	2.895(5)	O27−N23	2.872(5)
O7−N4	2.824(4)	O27−N24	2.774(4)

Hydrogen Bonds Associated with OH and Amide NH Groups

X−H···Y	X−H	Y···H	X···Y	X−H···Y
O7−H(O7)···O25	0.720(3)	2.102(3)	2.791(4)	160.2(2)
N3−H(N3)···O26	0.808(3)	2.062(2)	2.864(4)	171.9(3)
N4−H(N4)···O23	0.854(3)	2.140(2)	2.989(4)	172.5(2)
O27−H(O27)···Ow5	1.132(3)	1.705(3)	2.663(4)	138.8(2)
N23−H(N23)···O6	0.738(3)	2.228(3)	2.954(4)	168.0(2)
N24−H(N24)···O3	0.805(3)	2.133(3)	2.894(4)	157.6(2)

chelate molecules that are shown in parts A and B of Figure 5. In metal chelate A, a seven-coordination geometry is formed around the central metal ion. Six atoms from a ligand molecule form a trigonal prism around Mn1, and a water oxygen (Ow1) forms a cap above one of the square faces of the prism. In metal chelate B, five atoms from a ligand molecule and an oxygen atom from a water molecule are coordinated to Mn2 with the usual M−X distances. When an amide oxygen atom, O22, that is located at a distance of 3.188 Å from Mn2 is

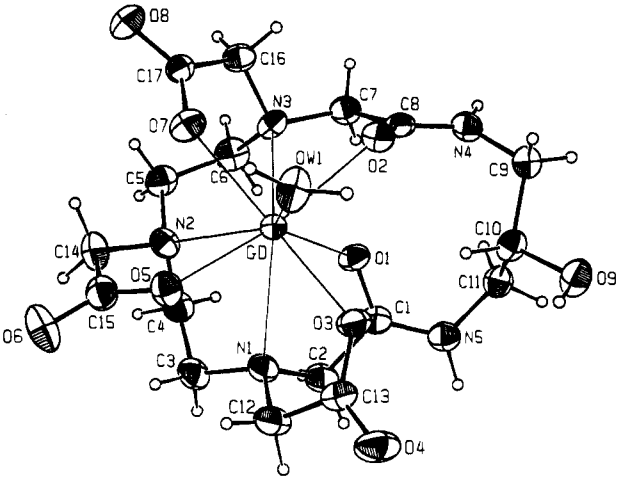

Figure 6. Molecular structure of a [Gd(16dtpapnOH)(H_2O)] chelate molecule. The atoms are shown at a 50% probability level. The coordination geometry around the central metal ion is a tricapped-trigonal prism.

included, the coordination geometry is described as a distorted capped-trigonal prism. The oxygen atom O22 is, however, too distant from the metal ion to be included in the first coordination sphere. The six coordinated atoms in the first coordination sphere form a quasi-trigonal prism, which is highly distorted from the D_{3h} symmetry. This structure is similar to that of [Mn(13edtapn)(H_2O)] in which two amide oxygen atoms are located at 2.142 and 3.122 Å, respectively, from the Mn atom.[19]

The difference between the coordination geometries of the two molecules is due to the different modes of coordination of amide oxygen atoms. The coordination of two amide oxygen atoms in molecule A results in the elongation of the Mn1−N1 bond, which is longer by 0.2 Å than the Mn2−N21 distance. All the atoms in a −C·NH·CO·C− moiety are on the same plane owing to the partial double bond character of the N−C bond (Table 2), and the dihedral angle between the two least squares planes of the amide groups is 41.09(9)° in molecule A and 30.0(2)° in molecule B. Interatomic distances between hydroxy oxygen atoms and amide nitrogen atoms are shown in Table 2. The O27−N24 distance, 2.774 Å, is significantly shorter than 2.9 Å predicted for an O−N van der Waals contact;[20] the other O−N pairs have a van der Waals contact distance of 2.9 Å. Each of the −OH and −CO−NH− groups forms intermolecular hydrogen bonds with oxygen atoms of the neighboring chelate or water molecules (Table 2), and no intramolecular hydrogen bond is formed between these groups. The close O27−N24 contact, therefore, originates from a direct interaction between the two atoms. The amide plane that includes N24 (*i.e.*, O21·N24·C21·C22·C29) orients favorably for the coordination of the amide oxygen atom O21 to Mn2, whereas the molecular plane of the other amide group in molecule B orients in such a way that the amide oxygen atom is directed away from the central metal ion. For molecule A, in which both amide oxygen atoms are coordinated to a central metal ion, the shorter Mn−O distance is found for the amide group whose amide nitrogen has a closer contact with a hydroxy oxygen atom. An OH group plays an important role in defining the coordination geometries in molecules A and B.

Structure of Gd(16dtpapnOH)·4H_2O. Table 3 shows selected interatomic distances. The molecular structure is shown in Figure 6. Two amide C=O groups and three carboxymethyl

(19) Inoue, M. B.; Oram, P.; Andreu-de-Riquer, G.; Inoue, M.; Borbat, P.; Raitsimring, A.; Fernando, Q. *Inorg. Chem.* **1995**, *34*, 3528.
(20) Pauling, L. *The Nature of the Chemical Bond*, 3rd ed.; Cornell University Press: New York, 1960; p 260.

Table 3. Selected Geometrical Parameters for Gd(16dtpapnOH)·4H_2O

Bond Distances (Å)			
Gd−O1$_{amide}$	2.439(3)	Gd−N1$_{amine}$	2.783(3)
Gd−O2$_{amide}$	2.454(2)	Gd−N2$_{amine}$	2.643(3)
Gd−O3$_{carboxylate}$	2.357(2)	Gd−N3$_{amine}$	2.695(2)
Gd−O5$_{carboxylate}$	2.350(2)	Gd−Ow1	2.408(3)
Gd−O7$_{carboxylate}$	2.364(3)		
N4$_{amide}$−C8	1.310(4)	N5$_{amide}$−C1	1.325(5)
N4$_{amide}$−C9	1.495(5)	N5$_{amide}$−C11	1.462(5)
Averaged Gd−X Distances (Å)[a]			
Gd−O$_{amide}$	2.447(2.445)	Gd−N$_{amine}$	2.707(2.677)
Gd−O$_{carboxylate}$	2.357(2.365)	Gd−O$_{water}$	2.408(2.474)
Dihedral Angles (deg)[a]			
O1·N5·C1·C2·C11−O2·N4·C7·C8·C9			103.3(99.7)
N1·N3·Ow1−O1·O2·O3			7.3(7.3)
N1·N3·Ow1−O5·O7·N2			4.8(5.6)

Hydrogen Bonds Associated with Hydroxy and Amide Groups

X−H···Y	X−H	H···Y	X···Y	X−H···Y
O9−H(O9)···Ow2	0.787(2)	1.979(3)	2.758(3)	170.5(2)
Ow1−H(w1a)···O9	0.947(3)	1.784(3)	2.728(4)	174.8(2)
N4−H(N4)···O8′	0.950(3)	2.065(3)	2.827(4)	136.0(2)
N5−H(N5)···O6′	0.950(4)	2.055(3)	2.914(4)	149.5(2)

[a] The corresponding values of Gd(16dtpapn)·4H_2O are shown in parentheses for comparison (ref 4).

groups are located on the same side with respect to the molecular plane of the macrocyclic ring, and all the donor groups are coordinated to a Gd atom. The five oxygen atoms, three amine nitrogen atoms from the same ligand molecule, and a water oxygen atom form a tricapped-trigonal prism around the central metal ion. The molecular structure is quite similar to that of [Gd(16dtpapn)(H_2O)];[4] the averaged Gd−X distances for carboxymethyl oxygen, amide oxygen, and amine nitrogen atoms are almost identical in the two metal chelates (Table 3). The only significant difference is that the Gd−Ow distance in Gd(16dtpapnOH) is shorter than that in Gd(16dtpapn). The OH group in Gd(16dtpapnOH)·4H_2O is equatorial without significant intramolecular O−N contacts with amide groups: O9−N4 = 3.713(4) Å and O9−N5 = 3.299(4) Å. The amide and hydroxy groups form reasonably strong hydrogen bonds with adjacent chelate molecules and water molecules (Table 3).

Discussion

The results of the ^1H NMR studies show that the introduction of an OH group increases the rigidity of the macrocyclic ring; on the other hand, the basicities of the donor atoms are not affected to a significant extent. The increase in the rigidity is caused by interaction between hydroxy and amide groups. This interaction may be more pronounced in the macrocycle with a smaller ring size. In fact, it plays an especially important role in defining the coordination geometry in the Mn^{2+} complex.

The coordination polyhedron of the Mn^{2+} complex in the solid state is highly distorted because of the steric constraint of the coordinated ligand molecule. Such a distorted coordination geometry is expected to be retained in solution. The EPR spectrum observed for the Mn^{2+} complex in a 50% methanol glass matrix centered at $g \approx 2.01$ exhibits six hyperfine lines due to a coupling between the electron spin and the Mn nuclear spin. The peak heights of these hyperfine lines are strongly dependent on the m_I component of the nuclear spin quantum number I. At intermediate fields between the neighboring lines, additional signals were observed (the spectrum has been deposited as Supporting Information). These weak doublets originate from the so-called forbidden transitions of $\Delta m_I = \pm 1$.[21] These features of the EPR spectrum indicate the presence of the zero-field splitting caused by a high distortion of the ligand field around the Mn^{2+} ion.[21] In the glass matrix, in which the molecular structure formed in solution is quenched, the chelate molecule has a low symmetry, as expected from the structure in the solid state.

The NMR T_1 relaxivity of [Gd(16dtpapnOH)(H_2O)]^0 was determined to be $r_1 = 3.45\ s^{-1}\ mM^{-1}$ in 90% D_2O at 250 MHz and at a temperature of 23 °C. This value is slightly smaller than the value of $3.7\ s^{-1}\ mM^{-1}$ determined for [Gd(16dtpapn)(H_2O)]^0 under the same experimental conditions.[6] The T_1 relaxivity of a paramagnetic metal chelate is mainly governed by an exchange between a coordinated water molecule and surrounding water molecules in solution.[10] This exchange process is dependent on the mode of coordination of the water molecule and also the geometrical environment around the water molecule. A larger volume available for hydration to a Gd^{3+} ion leads to a larger hydration number and hence a larger T_1 relaxivity. The small difference in the relaxivities of the two Gd^{3+} complexes shows that the environment around a coordinated water molecule is almost identical in solution, although the water molecule is bound more strongly in [Gd(16dtpapnOH)(H_2O)]^0 than that in [Gd(16dtpapn)(H_2O)]^0 in the solid state. The T_2 relaxivity r_2 of [Gd(16dtpapnOH)(H_2O)]^0 was $4.4\ s^{-1}\ mM^{-1}$, which was identical to the value reported for the corresponding (16dtpapn)$^{3-}$ complex.[6] The dipole field strengths produced by the Gd^{3+} electron spin at positions of surrounding water molecules are almost identical in the solutions of the two complexes.

The water solubility of Gd(16dtpapnOH)·4H_2O (1.05 g in 100 g of water at 25 °C) is considerably lower than that reported for Gd(16dtpapn)·4H_2O (39 g in 100 g of water),[6] although the former metal chelate contains an additional hydrophilic group in the ligand. This difference in the solubilities was one of the motivations for our structural study of Gd(16dtpapnOH)·4H_2O. Contrary to our expectation, the structures of the two metal chelates in the solid state do not show any significant differences that might result in the difference in the solubilities. The high solubility of Gd(16dtpapn) is due to the presence of carboxymethyl and amide groups, which are hydrophilic and facilitate hydration of the metal chelate. A plausible explanation for the low solubility of Gd(16dtpapnOH) is that the hydroxy group orients in solution to form hydrogen bonds with amide groups. The resulting intramolecular hydrogen bonds reduce the effective hydrophilicity of the metal chelate, thereby leading to a low hydration and low water solubility. This conformation change should occur locally around a hydroxy group in such a way that the environment around a coordinated water molecule is not affected to a significant extent.

The physical and structural properties of the metal complexes with (13edtapnOH)$^{2-}$ and (16dtpapnOH)$^{3-}$ are governed in part by an interaction between hydroxy and amide groups. An interaction between functional groups in a ligand molecule is one of the factors that should be taken into account in the molecular design of new macrocycles that may be useful for studies of molecular recognition properties.

Supporting Information Available: Tables of positional and B parameters, anisotropic thermal parameters, additional bond lengths and angles, least squares planes, and intermolecular contacts and ORTEP diagrams of the unit cells for Mn(13edtapnOH)·4H_2O and Gd(16dtpapnOH)·4H_2O and the EPR spectrum of Mn(13edtapnOH) in a glass matrix (37 pages). Ordering information is given on any current masthead page.

IC950733Y

(21) (a) Kuska, H. A.; D'Itri, F. M.; Popov, A. I. *Inorg. Chem.* **1966**, *5*, 1272. (b) Goodman, B. A.; Raynor, J. B. In *Advances in Inorganic Chemistry and Radiochemistry*; Emeléus, H. J., Sharpe, A. G., Eds.; Academic Press: New York, 1970; p 220.